LETTER TO THE JOURNAL

CANCER
COMMUNICATIONS
Open Access

Deletion of epithelial HKDC1 decelerates cellular proliferation and impairs mitochondrial function of tumorous epithelial cells thereby protecting from intestinal carcinogenesis

A metabolic switch favoring glycolysis over aerobic oxidative phosphorylation, termed the "Warburg effect", is a hallmark of cancer cells [1]. Hexokinase (HK) catalyzes the first and irreversible step of glycolysis, thereby limiting overall glycolytic activity. Mammals encode five HK family members: HK1-4 and HKDC1 (HK domain containing 1). HKDC1 has an exceptionally low glucose affinity and, therefore, low hexokinase activity under physiological conditions [2], raising questions about its function. A recent study indicated that HKDC1 functions as a glucose sensor within the tumor microenvironment [3], and its dysregulated expression has been associated with chronic inflammation [4] and various cancers [5]. Notably, HKDC1 promotes tumor immune evasion during immunotherapy in hepatocellular carcinoma patients [6], and blocking HKDC1 prevents disease progression in hepatic carcinoma, T cell lymphoma, and lung adenocarcinoma [7, 8]. However, its role in colorectal cancer (CRC) remains unknown. Here, we functionally investigated the role of HKDC1 in intestinal carcinogenesis.

First, we analyzed HKDC1 expression in the intestinal mucosa of healthy controls (HC) and CRC patients, as well as in various tumor tissues, using transcriptomic data from the human protein atlas (HPA) (https://www.proteinatlas.org) and The Cancer Genome Atlas (TCGA) (https://www.cancer.gov/ccg/research/genome-sequencing/tcga). Across different organs, HKDC1 showed the highest expression levels in the gastrointestinal tract (Supplementary Figure S1A), suggesting a potential role in intestinal function. Among various cancer types, HKDC1 expression was highest in CRC, followed by pancreatic, renal, stomach, and liver cancer (Supplementary Figure S1B). HKDC1 expression was significantly elevated in the intestinal mucosa of CRC patients compared to HC (Figure 1A) and in paired tumor versus normal tissue of the same CRC patients (Figure 1B). This overexpression appears to be more pronounced in tumor tissue, suggesting a potential association with cancer development rather than a general disease-related effect.

We then generated HKDC1-deficient human (Caco-2) and murine (CMT-93) colonic epithelial cell lines using CRISPR/Cas9 technology, and intestinal organoids, to investigate the role of HKDC1 in proliferation and cell death susceptibility in vitro, since uncontrolled cell division and resistance to cell death are hallmarks of cancer cells. Both Caco-2 and CMT-93 cells express HKDC1, HK1, and HK2, but with differential expression patterns (Supplementary Figure S2). Wildtype (WT) and HKDC1-deficient cells were seeded at equal densities, and after four days, cell growth was assessed using a colony-forming assay or protein quantification as a molecular measure of cell number. HKDC1-deficient cells displayed significantly reduced cell counts and protein content compared

List of abbreviations: ADP, Adenosine diphosphate; ANOVA, Analysis of variance; ANT2, Adenine nucleotide translocator 2; $Apc^{Min/+}$, Adenomatous-polyposis-coli multiple intestinal neoplasia; ATP, Adenosine triphosphate; ATP5A1, ATP Synthase Subunit Alpha 1; CRC, Colorectal cancer; DAPI, 4′,6-diamidino-2-phenylindole; Dpi, Days post infection; ECAD, E-Cadherin; FACS, Fluorescence activated cell sorting; FKPM, Median Fragments Per Kilobase of exon per Million reads; GCK, Glucokinase; GFPT1, Glutamine-Fructose-6-Phosphate Transaminase 1; GTEx, The Genotype-Tissue Expression; HC, Healthy controls; HK, Hexokinase; HKDC1, Hexokinase domain containing 1; HPA, Human Protein Atlas; IEC, Intestinal epithelial cell; IFN-β, Interferon beta; MPTP, Mitochondrial permeability transition pore; NSG, NOD.Cg-Prkdc^{SCID} Il2rg^{tm1Wjl}/SzJ; nTPM, normalized protein-coding transcripts per million; OCR, Oxygen consumption rate; RNA-seq, Ribonucleotide acid sequencing; SEM, Standard error of the mean; SLC25A5, Solute Carrier Family 25 Member 5; STRING, Search Tool for the Retrieval of Interacting Genes/Proteins; STS, Staurosporine; TCGA, The Cancer Genome Atlas; TMRM, Tetramethylrhodamine-methyl ester; TNF, Tumor necrosis factor; TUNEL, Terminal deoxynucleotidyl transferase dUTP nick end labelling; VDAC, Voltage-dependent anion channel; WT, Wildtype.
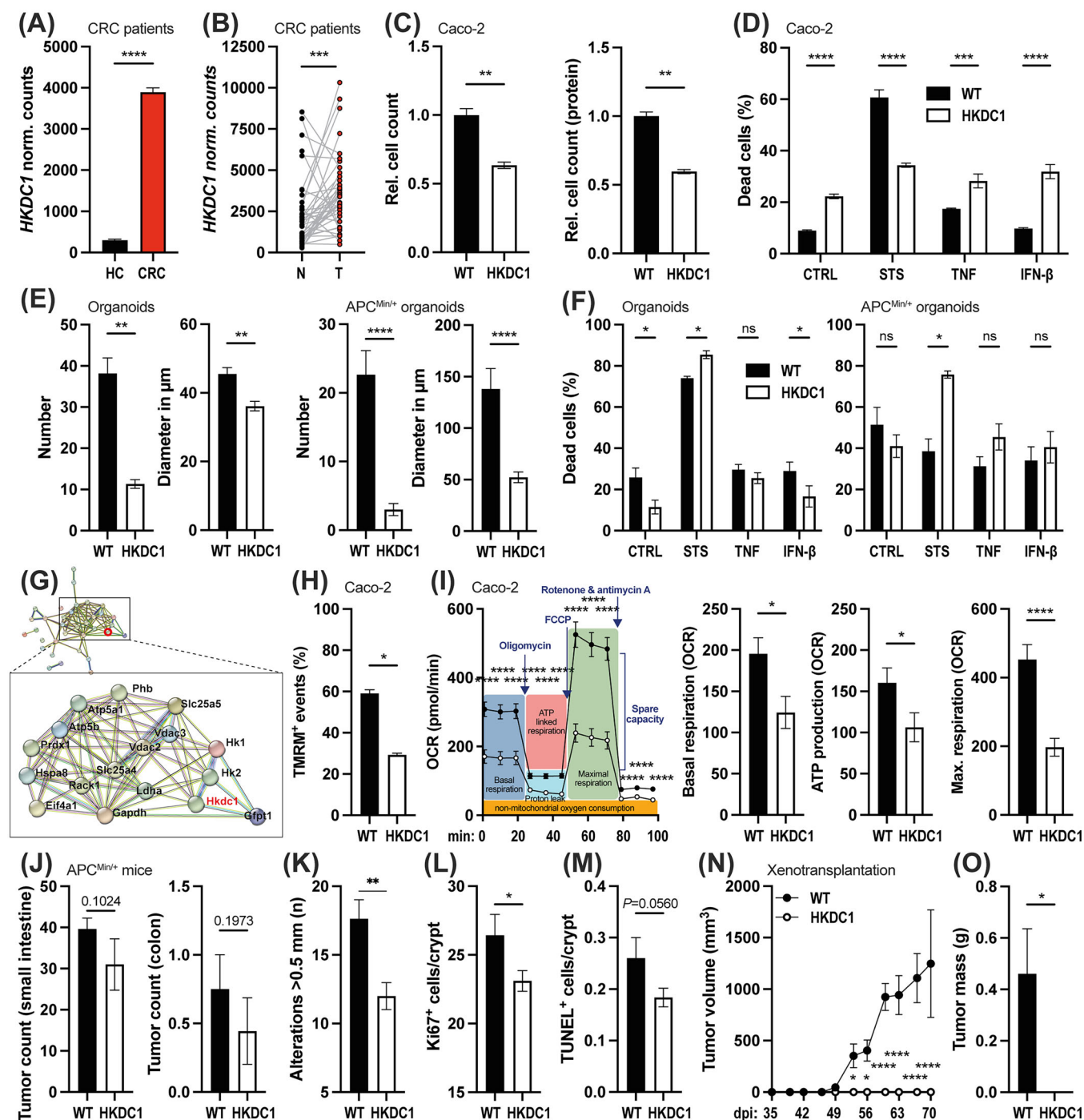
FIGURE 1 *HKDC1* expression is associated with colorectal cancer. (A) *HKDC1* expression (normalized counts) in the intestinal mucosa of healthy controls (HC) and CRC patients, retrieved from The Genotype-Tissue Expression (GTEx, https://gtexportal.org, $n = 454$ samples) and TCGA ($n = 651$ samples). (B) *HKDC1* expression in paired normal (N) and tumor (T) tissues of $n = 41$ CRC patients from TCGA. *** $P < 0.001$, Wilcoxon rank test. (C-F) HKDC1 deletion alters proliferation and cell death. Proliferation, measured by cell count four days post-seeding or by protein amount, was reduced in HKDC1-deficient human Caco-2 cells(C) ($n = 4 - 6$ per group). WT and HKDC1-deficient Caco-2 cells were stimulated with either staurosporine(D) (STS, 10 μmol/L for Caco-2), tumor necrosis factor (TNF, 500 ng/μl), or interferon beta (IFN-β, 1000 U/μl) for 24 hours, and cell death was assessed through zombie staining and FACS analysis. $n = 5$ per group. HKDC1-deficient normal and tumorigenic $Apc^{Min/+}$ organoids exhibited reduced growth, as determined by an organoid forming assay (E). The number and diameter of organoids were measured five days after seeding ($n = 6 - 12$ per genotype and group). Percentage of dead cells in normal and tumorigenic $Apc^{Min/+}$ organoids after stimulation with STS, TNF, or IFN-β for 24 hours (F) ($n = 5$ per group). (G-I) HKDC1 deficiency impairs mitochondrial function. Network of HKDC1 interaction partners based on STRING analysis of proteins identified from HKDC1 immunoprecipitation of intestinal mucosa, highlighting a cluster of mitochondria-related proteins (G). Nodes represent individual proteins. Lines indicate known (cyan = curated databases, magenta = experimentally determined) and predicted (green = gene

to WT cells (Figure 1C, Supplementary Figure S3A), indicating that HKDC1 contributes to cellular proliferation. To investigate whether HKDC1 affects sensitivity to cell death induction, WT and HKDC1-deficient Caco-2 and CMT-93 cells were stimulated with cell death-inducing agents, and cell viability was analyzed. Under all conditions, except for staurosporine-treated Caco-2 cells, HKDC1-deficient cells showed a higher percentage of dead cells than WT controls (Figure 1D, Supplementary Figure S3B). These findings suggest that HKDC1 loss influences the cell death response in cancerous epithelial cells, potentially by affecting mitochondria-dependent cell death. No compensatory upregulation of HK1 or HK2 was observed in HKDC1-deficient cells (Supplementary Figure S3C), although off-target effects of staurosporine cannot be ruled out due to its non-selective protein kinase inhibitor activity. These findings were further validated *ex vivo* using non-transformed intestinal epithelial organoids. HKDC1-deficient organoids were derived from $Hkdc1^{\Delta IEC}$ mice (Supplementary Figure S4), which carry a *Hkdc1* deletion specifically in intestinal epithelial cells (IECs). Organoid formation assays revealed that HKDC1-deficient organoids grew more slowly and exhibited reduced overall cell mass compared to WT organoids (Figure 1E). To assess the impact of HKDC1 loss in intestinal tumorigenesis, $Hkdc1^{\Delta IEC}$ mice were crossbred with tumor-bearing $Apc^{Min/+}$ mice, a model of sporadic intestinal carcinogenesis [9]. HKDC1-deficient $Apc^{Min/+}$ organoids, derived from intestinal tissue including tumors, also showed slower growth and reduced cell mass compared to controls (Figure 1E). Treatment with staurosporine, which triggers cell death via mitochondrial cytochrome c release, induced cell death in normal organoids regardless of HKDC1

genotype. However, while WT $Apc^{Min/+}$ tumor organoids were completely resistant to cell death, HKDC1 deletion restored cell death susceptibility (Figure 1F). Transcriptional profiling and gene ontology enrichment analysis revealed alterations in proliferation and cell death pathways, as well as metabolic and immune processes, in HKDC1-deficient $Apc^{Min/+}$ organoids compared to WT controls (Supplementary Figure S5). Collectively, these data demonstrate that HKDC1 loss in colonic epithelial cells affects both proliferation and cell death dynamics.

Seeking a more comprehensive understanding HKDC1's role in cellular function, we performed HKDC1 immunoprecipitation. Lysates from the intestinal mucosa of $Hkdc1^{\Delta IEC}$ and WT mice were incubated with an HKDC1 antibody bound to Dynabeads, followed by washing, purification, and LC-MS analysis. After excluding cytoskeletal proteins, we identified 34 candidate HKDC1 interaction partners (Supplementary Table S1). A protein interaction network analysis revealed a distinct cluster of proteins associated with the regulation of mitochondrial membrane potential and pore activity (Figure 1G). This cluster included other HK isoforms, HK1 and HK2, as well as VDAC2 (Voltage-dependent anion channel 2), VDAC3, SLC25A5 (Solute Carrier Family 25 Member 5 or ADP/ATP Translocase 2), ATP5A1 (ATP Synthase Subunit Alpha 1), and GFPT1 (Glutamine-Fructose-6-Phosphate Transaminase 1). These proteins play roles in mitochondrial metabolism and the mitochondrial permeability transition pore (MPTP), although the exact composition of the MPTP remains unclear [10]. To investigate mitochondrial membrane potential, we used MitoProbe tetramethylrhodamine-methyl ester (TMRM). TMRM signals were consistently reduced in HKDC1-deficient

neighborhood, red = gene fusions, blue = gene co-occurrence) interactions. Mitochondrial phenotyping of WT and HKDC1-deficient human Caco-2 cells. Deletion of HKDC1 resulted in (H) reduced mitochondrial membrane potential, as measured by TMRM staining and FACS analysis, and (I) decreased oxygen consumption rate (OCR) as a measure of mitochondrial activity, determined by Seahorse Mito Stress metabolic analysis. Basal respiration, maximal respiration, and ATP production were significantly reduced in HKDC1-deficient cells. $n =$ 9 - 10 per genotype. (J-O) Epithelial deletion of *HKDC1* ameliorates intestinal carcinogenesis. (J-M) Sporadic intestinal tumorigenesis in the $Apc^{Min/+}$ mouse model. 20-week-old tumor-bearing $Apc^{Min/+}$-$Hkdc1^{\Delta IEC}$ mice were compared to WT littermate controls and analyzed for (J) tumor numbers, (K) the number of lesions > 0.5 mm, (L) proliferating (Ki67-positive), and (M) apoptotic (TUNEL-positive) colonic IECs. $n =$ 9 - 10 per genotype. *: $P < 0.05$, Mann-Whitney-U-test. (N-O) Xenograft model. NSG mice were injected with WT and HKDC1-deficient human Caco-2 cells, and tumor volume (mm^3) was monitored over time (N). At 70 days post-injection (dpi), the experiment was terminated for ethical reasons, and total tumor mass (g) was measured (O). $n = 4$ mice per injection group. *$P < 0.05$, **$P < 0.01$, ***$P < 0.001$, and ****$P < 0.0001$, Mann-Whitney-U-test or two-way ANOVA. All data are presented as mean ± SEM. ANOVA, Analysis of variance; Apc$^{Min/+}$, Adenomatous-polyposis-coli multiple intestinal neoplasia; ATP, Adenosine triphosphate; CRC, Colorectal cancer; Dpi, Days post infection; FACS, Fluorescence activated cell sorting; FKPM, Median Fragments Per Kilobase of exon per Million reads; GTEx, The Genotype-Tissue Expression; HC, Healthy controls; HK, Hexokinase; HKDC1, Hexokinase domain containing 1; HPA, Human Protein Atlas; IEC, Intestinal epithelial cell; IFN-β, Interferon beta; MPTP, Mitochondrial permeability transition pore; N, normal tissue; NSG, NOD.Cg-PrkdcSCID Il2rgtm1Wjl/SzJ; OCR, Oxygen consumption rate; SEM, Standard error of the mean; STRING, Search Tool for the Retrieval of Interacting Genes/Proteins; STS, staurosporine; T, tumor tissue; TCGA, The Cancer Genome Atlas; TMRM, Tetramethylrhodamine-methyl ester; TNF, Tumor necrosis factor; TUNEL, Terminal deoxynucleotidyl transferase dUTP nick end labelling; VDAC, Voltage-dependent anion channel; WT, Wildtype.

compared to WT cells, indicating a decrease in mitochondrial membrane potential in the absence of HKDC1 (Figure 1H, Supplementary Figure S6A). Additionally, Seahorse analyses were performed. Consistent with the findings from TMRM, HKDC1-deficient cells showed significantly reduced mitochondrial respiration (Figure 1I, Supplementary Figure S6B). Basal respiration along, along with ATP-linked and maximal respiration, was lower in HKDC1-deficient cells, highlighting a dysfunctional mitochondrial electron transport chain. Together, these data suggest a crucial role for HKDC1 in mitochondrial function, potentially due to its association with mitochondria and MPTP-related proteins.

To directly assess HKDC1's role in intestinal carcinogenesis in vivo, we phenotyped tumor-bearing $Apc^{Min/+}$-$Hkdc1^{\Delta IEC}$ mice. Although body and organ weights did not differ between $Apc^{Min/+}$-$Hkdc1^{\Delta IEC}$ and WT mice (Supplementary Figure S7), intestinal tumor counts in $Apc^{Min/+}$-$Hkdc1^{\Delta IEC}$ trended lower compared to WT mice, though this did not reach statistical significance ($P = 0.102$ for the small intestine and $P = 0.197$ for the colon (Figure 1J). This lack of significance may be due to technical limitations in identifying macroscopic tumors in the tissue. Further analysis showed that tumor burden, measured as the percentage of the affected area in intestinal Swiss rolls, did not differ between WT and $Apc^{Min/+}$-$Hkdc1^{\Delta IEC}$ mice. However, $Apc^{Min/+}$-$Hkdc1^{\Delta IEC}$ mice showed fewer lesions larger than 0.5 mm (Figure 1K), suggesting that HKDC1 may influence tumor growth rather than initiation. Supporting this, histological analyses of colon sections revealed a significant reduction in Ki67-positive proliferating IECs in $Apc^{Min/+}$-$Hkdc1^{\Delta IEC}$ mice (0.87-fold, $P = 0.038$) and a slight decrease in apoptotic TUNEL-positive IECs (0.71-fold, $P = 0.056$) (Figure 1L-M). To further corroborate these findings, we performed a xenograft transplantation model, where WT and HKDC1-deficient Caco-2 cells were subcutaneously injected into the flanks of immunocompromised NSG mice, and tumor growth was monitored over time. By 60 days post-injection (dpi), mice transplanted with WT cells began developing visible tumors, which continued to grow until 70 dpi. In stark contrast, none of the mice transplanted with HKDC1-deficient cells developed any detectable tumor (Figure 1N-O). Thus, deletion of HKDC1 in human colonic epithelial cells completely abolished their tumor-forming ability, providing full protection against cancer development. It is important to note that, despite similar physiological responses, differences exist among the models used. For example, CMT-93 and Caco-2 cell lines express different levels of HK family members, and the $Apc^{Min/+}$ model primarily represents small intestine-driven tumorigenesis due to an APC mutation in the Wnt signaling pathway, whereas our xeno-transplantation model used colonic epithelial cells to more closely resemble human CRC. Further investigations using additional models are needed to elucidate the underlying molecular mechanisms.

Our findings demonstrate that HKDC1 influences cancer cell proliferation, susceptibility to cell death, and ultimately intestinal carcinogenesis, potentially through interactions with mitochondrial proteins regulating membrane permeability. However, the precise molecular mechanism remains unclear. Collectively, our data highlight the significance of HKDC1 in CRC pathobiology, presenting it as a promising target for further investigation and potential therapeutic interventions. However, further studies are required to uncover the molecular mechanisms by which HKDC1 affects cellular physiology and to access the feasibility and efficacy of HKDC1-targeted interventions for CRC.

DATA AVAILABILITY STATEMENT

All data is either included in this manuscript or deposited on public databases. The RNA sequencing data are accessible through the European Nucleotide Archive (https://www.ebi.ac.uk/ena) under the accession number PRJEB82610.

ETHICS APPROVAL AND CONSENT TO PARTICIPATE

All animal experiments were approved by the local animal safety review board of the federal ministry of Schleswig Holstein and conducted according to national and international laws and policies (approval numbers: V242-56302/2018[100-11/18] and IX552-65205/2024[24-4/24]). No human studies were conducted but only data from public databases used.

Lea Järke[1]
Saskia Weber-Stiehl[1]
Kensuke Shima[2]
Karlis Arturs Moors[3]
Jerome Genth[3]
Fenja Amrei Schuran[1]
Lena Best[3]
Markus Tschurtschenthaler[4,5,6]
Burkhardt Flemer[1]
Silke Lüschen[7]
Christoph Röcken[7]
Andreas Tholey[3]
Christoph Kaleta[3]
Jan Rupp[2,8,9]
Philip Rosenstiel[1]
Felix Sommer[1]

[1] Institute of Clinical Molecular Biology, Kiel University, Kiel, Germany
[2] Institute of Medical Microbiology, University of Lübeck, Lübeck, Germany
[3] Institute of Experimental Medicine, Kiel University, Kiel, Germany
[4] Translational Cancer Research and Institute of Experimental Cancer Therapy, Klinikum rechts der Isar, School of Medicine and Health, Technical University of Munich, Munich, Germany
[5] Center for Translational Cancer Research (TranslaTUM), Klinikum rechts der Isar, School of Medicine and Health, Technical University of Munich, Munich, Germany
[6] Division of Translational Cancer Research, German Cancer Research Center (DKFZ) and German Cancer Consortium (DKTK), Heidelberg, Germany
[7] Department of Pathology, University Hospital Schleswig-Holstein, Campus Kiel, Kiel, Germany
[8] Infectious Disease Clinic, University Hospital Schleswig-Holstein/Campus Lübeck, Lübeck, Germany
[9] German Center for Infection Research (DZIF), Partner Site Hamburg-Lübeck-Borstel-Riems, Lübeck, Germany

Correspondence

Felix Sommer; Institute of Clinical Molecular Biology (IKMB), Christian-Albrechts-University (CAU) Kiel, Rosalind-Franklin-Str. 12, Kiel D-24105, Germany.
Email: f.sommer@ikmb.uni-kiel.de

Lea Järke and Saskia Weber-Stiehl contributed equally with shared first authorship.

Kensuke Shima, Karlis Arturs Moors, and Jerome Genth contributed equally with shared second authorship.

ORCID

Markus Tschurtschenthaler https://orcid.org/0000-0002-0060-4790
Felix Sommer https://orcid.org/0000-0002-6545-3487

REFERENCES

1. Hanahan D, Weinberg RA. Hallmarks of Cancer: The Next Generation. Cell. 2011;144:646–74.
2. Hayes MG, Urbanek M, Hivert M-F, Armstrong LL, Morrison J, Guo C, et al. Identification of HKDC1 and BACE2 as genes influencing glycemic traits during pregnancy through genome-wide association studies. Diabetes. 2013;62:3282–91.
3. Liu P, Luo Y, Wu H, Han Y, Wang S, Liu R, et al. HKDC1 functions as a glucose sensor and promotes metabolic adaptation and cancer growth via interaction with PHB2. Cell Death Differ. 2024;31:1595–610.
4. Häsler R, Feng Z, Bäckdahl L, Spehlmann ME, Franke A, Teschendorff A, et al. A functional methylome map of ulcerative colitis. Genome Res. 2012;22:2130–7.
5. Khan MdW, Terry AR, Priyadarshini M, Ilievski V, Farooq Z, Guzman G, et al. The hexokinase "HKDC1" interaction with the mitochondria is essential for liver cancer progression. Cell Death Dis. 2022;13:660.
6. Zhang Y, Wang M, Ye L, Shen S, Zhang Y, Qian X, et al. HKDC1 promotes tumor immune evasion in hepatocellular carcinoma by coupling cytoskeleton to STAT1 activation and PD-L1 expression. Nat Commun. 2024;15:1314.
7. Chen Q, Feng J, Wu J, Yu Z, Zhang W, Chen Y, et al. HKDC1 C-terminal based peptides inhibit extranodal natural killer/T-cell lymphoma by modulation of mitochondrial function and EBV suppression. Leukemia. 2020;34:2736–48.
8. Wang X, Shi B, Zhao Y, Lu Q, Fei X, Lu C, et al. HKDC1 promotes the tumorigenesis and glycolysis in lung adenocarcinoma

via regulating AMPK/mTOR signaling pathway. Cancer Cell Int. 2020;20:450.

9. Moser AR, Pitot HC, Dove WF. A Dominant Mutation That Predisposes to Multiple Intestinal Neoplasia in the Mouse. Science. 1990;247:322–4.

10. Baines CP, Gutiérrez-Aguilar M. The still uncertain identity of the channel-forming unit(s) of the mitochondrial permeability transition pore. Cell Calcium. 2018;73:121–30.

SUPPORTING INFORMATION

Additional supporting information can be found online in the Supporting Information section at the end of this article.